Chiral Quantum Dots

DOI: 10.1002/anie.201103762

Optical Coupling Between Chiral Biomolecules and Semiconductor Nanoparticles: Size-Dependent Circular Dichroism Absorption**

Yunlong Zhou, Zhening Zhu, Wenxiao Huang, Wenjing Liu, Shaojue Wu, Xuefeng Liu, Yan Gao, Wei Zhang, and Zhiyong Tang**

Colloidal semiconductor nanoparticles, which are also called as quantum dots (QDs) when their sizes fall to the range of 1–10 nm, are receiving widespread attention for uses in optical and biological materials owing to their distinct size-dependent absorption and emission properties.[1] By manipulating synthesis and assembly processes, recent studies have revealed many novel properties and applications of QDs.[2] Among those, studies on nanoscale chirality are especially interesting.[3] However, little attention has been paid to their chiral optical properties originated from quantum effects.[4] The study of chirality at nanoscale is one of the most intriguing research topics in many fields of biology, physics, chemistry, and materials.[5] For example, chiral inorganic nanoparticles (NPs) or QDs are not only appropriate building blocks to fabricate negative-refractive index metamaterials in the visible-light region, but are also expected to work as artificial proteins for chiral catalysis or inhibition of specific enzymes.[6]

Recently, encouraged by theoretical and application significance,[7] considerable progress has been made on the synthesis of different types of chiral metal NPs and QDs, as well as the understanding of chiral origin of such inorganic nanomaterials.[3b,4b,8] In contrast, the investigation of chiral optical properties of chiral NPs or QDs normally showed broad circular dichroism (CD) absorption features in the region of 200–500 nm, which originates from the chiral surface defects of QDs.[8d,e] Furthermore, theoretical calculations based on the model of chiral nanoclusters predicted that broad CD absorption peaks resulted from Coulomb dipole–dipole interactions between chiral molecules and QDs.[9] Nevertheless, unlike conventional size-dependent absorption and luminescence characteristics of QDs that arise from quantum confinement effects, size-dependent chiral properties from QDs have not yet been observed. Having the ability to adjust chiral properties by tuning the size of QDs would improve the possibility of using chiral inorganic nanomaterials for many applications.

The question arises as to whether the broad CD absorption features of chiral QDs can be manipulated through modulation of their intrinsic properties. To answer this critical question, herein we prepared CdTe and CdSe QDs stabilized by chiral biomolecules, including glutathione (GSH) and cysteine (CYS), and studied their chiral optical properties. We observed and confirmed the size-dependent CD absorption of QDs in the visible-light region from both experimental and theoretical aspects. This work will greatly contribute to the study of nanoscale chirality.

First, CdTe QDs stabilized by (D,L)-GSH were prepared in aqueous solution according to a method modified from the literature.[2b] By altering the reaction duration, CdTe QDs can be synthesized with desirable sizes. Owing to the different absorption strengths of QDs and stabilizers (Figure 1c), we separately measured CD signals at the characteristic wavelength of chiral stabilizers and QD cores using QDs solutions with different concentrations. Furthermore, to exclude possible interference of free Cd ions and $Cd_x(GSH)_y$ complexes in solution, all the crude QDs solutions were subjected to repetitive centrifugation to remove them thoroughly. As shown in Figure 1a,b, the optically active GSH and $Cd_x(GSH)_y$ complexes contribute CD signals only in the UV region where the wavelength is shorter than 260 nm. Compared with pure GSH (Figure 1a), there is an obvious change in CD signals, with an additional peak appearing at about 240 nm for $Cd_x(GSH)_y$ complexes (Figure 1b) and GSH-stabilized CdTe QDs (Figure 1c). Notably, when the concentrations of QDs are increased about 30 times relative to those in Figure 1c, new CD peaks with opposite signs are easily observed in the range of 400–700 nm for the D-GSH-stabilized CdTe QDs (Figure 1d) and L-GSH-stabilized CdTe QDs (Figure 1e).

More interestingly, for both D- and L-GSH-stabilized CdTe QDs, such characteristic CD absorption peaks in the range of 400–700 nm exhibit gradual bathochromic shifts along with the first excitonic absorption bands when the sizes of QDs increase with the reaction time (Figure 1d,e). The size-dependent red-shifts in both CD signals and UV/Vis spectra clearly point to the quantum confinement effect of QDs. It should also be noted that at the same reaction time,

[*] Y. Zhou, Z. Zhu, W. Huang, W. Liu, S. Wu, X. Liu, Prof. Y. Gao, Prof. Z. Tang
Laboratory of Nanomaterials
National Center for Nanoscience and Technology
Beijing 100190 (P. R. China)
E-mail: zytang@nanoctr.cn
Prof. W. Zhang
Institute of Applied Physics and Computational Mathematics
Beijing 100088 (P. R. China)
E-mail: zhang_wei@iapcm.ac.cn

[**] This work was partially supported by the National Natural Science Foundation for Distinguished Youth Scholars of China (21025310, Z.Y.T.), the National Natural Science Foundation of China (20973047, Z.Y.T.; 10874020, W.Z.), the National Research Fund for Fundamental Key Project (2009CB930401, Z.Y.T.; 2011CB922204, W.Z.), the China–Korea Joint Research Project (2010DFA51700, Z.Y.T.), and the 100-Talent Program of the Chinese Academy of Sciences (Z.Y.T.).

Supporting information for this article is available on the WWW under http://dx.doi.org/10.1002/anie.201103762.

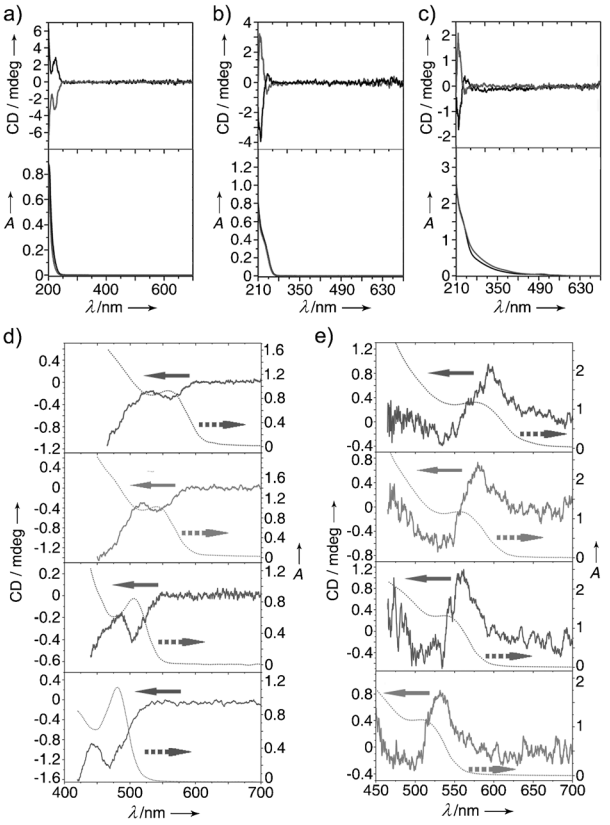

Figure 1. CD spectra and corresponding UV/Vis spectra of a) D-GSH (black) and L-GSH (gray); b) Cd_x(D-GSH)$_y$ (black) and Cd_x(L-GSH)$_y$ (gray) complexes, pH 11.2; c) D-GSH-stabilized CdTe QDs (black) and L-GSH-stabilized CdTe QDs (gray). d,e) Size-dependent CD spectra (——) and corresponding UV/Vis spectra (•••••) of D-GSH-stabilized CdTe QDs (d) and L-GSH-stabilized CdTe QDs (e). The data in (d) and (e) were obtained when concentrations of QDs were about 30 times higher than those in (c); the preparation time from bottom to top was 30 min, 60 min, 120 min, and 180 min, respectively.

the growth rate of D-GSH-stabilized CdTe QDs is slower than that of L-GSH-stabilized CdTe QDs, leading to CD signals and UV/Vis absorption peaks with shorter wavelength (Figure 1 d,e; Supporting Information, Figure S2). A similar difference in growth kinetics of QDs induced by chiral stabilizers has been reported and elucidated in our previous work.[8e] The difference in growth kinetics also results in non-mirror-image symmetry of the CD spectra of (D,L)-GSH-stabilized CdTe QDs (Figure 1 d,e). To quantify the size effect on the optical activity of chiral GSH-stabilized CdTe QDs, we further calculate the peak values of maximum anisotropic factor (g factor) that are defined as $\Delta\varepsilon/\varepsilon$ (here $\Delta\varepsilon=\varepsilon_L-\varepsilon_R$ and $\varepsilon=\varepsilon_L+\varepsilon_R$, respectively, where ε is molar extinction coefficient).[10] As shown in Table 1, the typical g factors of CdTe QDs stabilized with (D,L)-GSH are in the range of -3.6×10^{-5} to $+3.1\times10^{-5}$, respectively, and the values gradually decrease with the increase of QD sizes (for a detailed size estimation, see the Supporting Information, p. S5). A similar tendency has been observed in metal nanoclusters, for which larger species have a smaller optical activity.[8a]

Table 1: MAFs of (D,L)-GSH-stabilized CdTe QDs of different size at the corresponding CD peak.[a]

	D-GSH-CdTe QDs				L-GSH-CdTe QDs			
CD peak [nm]	469	519	541	560	536	561	583	594
MAF ($g\times10^{-5}$)	−3.6	−3.0	−1.5	−1.0	+3.1	+3.2	+2.4	+2.2
Size [nm]	2.7	3.0	3.5	3.8	3.0	3.5	3.8	4.2

[a] MAF = maximum anisotropic factor.

Theoretical studies were carried out to establish the origin of the novel and size-dependent CD signals in the range of 400 nm to 700 nm, where chiral molecules show no measurable CD signals. The calculations were performed based on the discrete dipole approximation method,[11] considering that one chiral molecule with polarizabilities α_1^L and α_1^R (for left- and right-polarized light) is coupled with an achiral quantum dot with polarizability α_2 (same for left- and right-polarized light; see the detailed calculation in the Supporting Information, p. S7–S9). The interaction between the chiral molecule and QD leads to the dipoles p_j, $j=1$, 2 [Supporting Information, Eq. (S3)]. Thus, we can see that the effective polarizability for a QD is a mixture of bare polarizabilities (α_2, $\alpha_1^{L/R}$) for both QD and the chiral molecule. As the polarizability of a chiral molecule depends on the polarization of light, the effective polarizability of a QD is also polarization-dependent owing to the coupling to the chiral molecule, which leads to the CD signals for QDs observed in experiments. Moreover, seen from the Supporting Information, Equation (S5), it is clear that the strength of CD signals is mainly determined by the product of α_2 and $\alpha_1^L-\alpha_1^R$. Therefore, the origin of the novel CD spectra is the combination of the optical activity (though very weak at 400 nm to 700 nm) of the chiral molecule and the dramatic enhancement effects from the strong absorption of QDs. This conclusion is supported by the fact that the CD peak in experiments appears at the region of wavelength where the absorption shows dramatic changes (Figure 1 d,e).

More theoretical results are presented in Figure 2 for further comparison with the experimental observations. The theoretically calculated CD spectra for D-GSH-stabilized CdTe QDs in Figure 2 a look very similar with those in Figure 1 c, showing significant CD signals in the UV region (200–250 nm). Moreover, the peak positions appear at 215 nm/243 nm (the ratio of peak values is −4.4), which is close to the experimental results in Figure 1 c (218 nm/240 nm; ratio of peak values −4.0). Under this condition, the CD signal in the visible light region is too weak to be observed. Yet, appreciable CD could be observed for high concentrations of QDs owing to the large enhancement effect [Supporting Information, Eq. (S5)]. In Figure 2 b–e, all the CD and absorption spectra for different-sized QDs at a high concentration (30 times higher than those in Figure 1 c and Figure 2 a) show similar lineshapes overall as the curves as in Figure 1 d. Up to an overall constant, the theoretical results for g factors are -2.1×10^{-5} (at peak position 473 nm), -1.5×10^{-5} (at peak position 513 nm), -1.2×10^{-5} (at peak position 540 nm), and -1.0×10^{-5} (at peak position 557 nm). These theoretical results are in semi-quantitative agreement with experimental observations (Table 1). Both experimental and theoretical results clearly reveal the size-dependence (owing to confinement) of CD characteristics in the visible-light

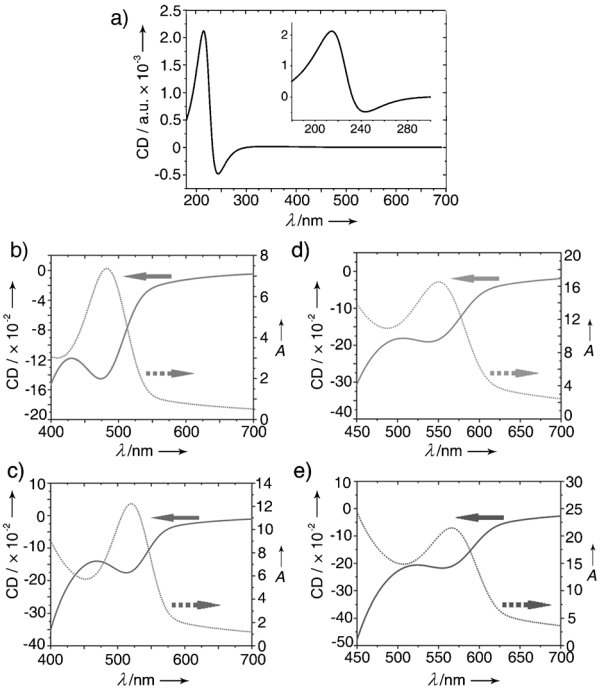

Figure 2. Calculated CD spectra of a) D-GSH stabilized CdTe QDs at low concentration, and b–e) size-dependent CD spectra (——) and corresponding UV/Vis spectra (•••••) of D-GSH-stabilized CdTe QDs of different sizes at high concentrations. The inset in (a) shows the enlarged part in the UV light region.

region (Figure 1 d, Figure 2 b–e), including the peak positions and the g factors.

However, the optical coupling between chiral stabilizers and QDs cores is ubiquitous in nanoscale hybrid systems. To testify the generality, QDs with different chiral stabilizers (CYS-stabilized CdTe) or different core components (CYS-stabilized CdSe) were prepared.[2b,12] Evidently, similar size-dependent chiral effects are found in the CD spectra of both QDs (Figure 3; Supporting Information, Table S1 and S2). With the increase of QD sizes, a gradual red-shift of CD signals along with the UV/Vis absorption peaks are observed for both (D,L)-CYS-stabilized CdTe QDs (Figure 3 a,b) and CdSe QDs (Figure 3 c,d). In contrast to GSH-stabilized CdTe QDs, both CYS-stabilized CdTe QDs and CdSe QDs show obvious bisignated CD signals in the range of the first excitonic transition band. Theoretically, in an exciton couplet, bisignated CD bands of opposite signs should be resolved. However, the two corresponding CD absorption bands are normally separated by only a few or a few ten nanometers, and they may not be resolved because of an electrically allowed transition or they may be forbidden.[10] Therefore, the appearance of multiple CD peaks for (D,L)-CYS-stabilized CdTe QDs could be attributed to hybridization of the QD state with molecular states of CYS with multiple CD bands. Furthermore, the g factors for both CYS-stabilized CdTe QDs and CdSe QDs are in the range of -9×10^{-5}–$+6\times10^{-5}$, and generally the values decrease with increase of QD sizes (Supporting Information, Table S1 and S2). This result is also consistent with that obtained from GSH-stabilized CdTe QDs.

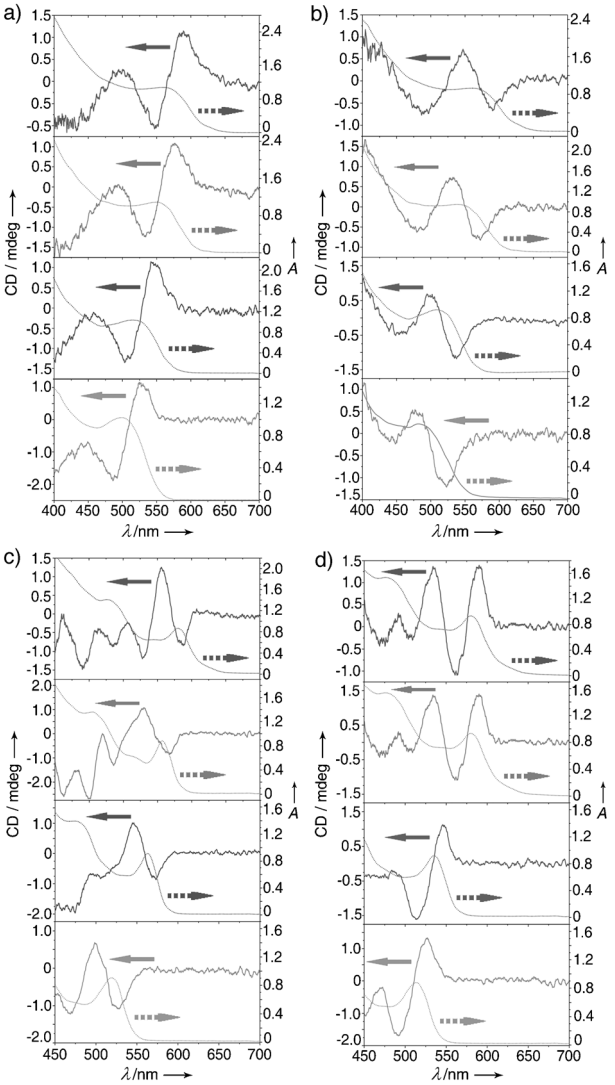

Figure 3. Size-dependent CD spectra (——) and corresponding UV/Vis spectra (•••••) of D-CYS-stabilized CdTe QDs (a), L-CYS-stabilized CdTe QDs (b), D-CYS-stabilized CdSe QDs (c), and L-CYS-stabilized CdSe QDs (d). The spectra (from top to bottom) for each part in (a)–(d) correspond to an increase in size of the QDs.

In summary, we have presented a new type of size-dependent nanoscale optical properties, CD absorption, along with conventional absorption and photoluminescence. This quantum confinement of CD in the visible-light region is demonstrated by a combination of the optical activity of chiral molecules and the strong absorption of QDs. These results not only highlight the importance of the classical quantum confinement, but also put the first step of approaching nanoscale chiral photonics, which are of great significance in both fundamental research and practical applications.

Experimental Section

Synthesis of biomolecule-stabilized CdTe QDs:[2b] Briefly, Cd-$(ClO_4)_2\cdot6H_2O$ (0.59 mmol) and (D,L)-GSH (1.43 mmol; see the Supporting Information, Figure S1) or CYS were dissolved in deionized water (32 mL), followed by adjusting the pH value to

11.2 with 1M NaOH. The solution was placed in a three-necked flask and deaerated by N_2 for 0.5 h. Then, H_2Te (generated by the reaction of 0.05 g Al_2Te_3 lumps with 4 mL of 0.5 M H_2SO_4 under a N_2 atmosphere) was passed through to the N_2-saturated aqueous solution from above. The CdTe QDs with different sizes could be obtained by refluxing the solution in 100 °C oil bath for different periods of reaction time.

Synthesis of CdSe QDs stabilized by stearic acid (SA):[12] The synthesis of SA-stabilized CdSe QDs was followed by a modified literature method: $Cd(SA)_2$ (1.14 mmol) and selenium powder (0.3525 mmol) were added into a three-necked round-bottom flask containing 1-octadecene (ODE; 5 mL). Subsequently, five argon–vacuum cycles and vacuum treatment for 10 min were performed to remove excess oxygen and water. Finally, the solution was further heated to 240 °C at a heating rate of 10 °C min^{-1} under a flow of argon. The reaction was monitored by UV/Vis spectroscopy by taking aliquots from the solution. SA-stabilized CdSe QDs having different sizes were chosen for ligand exchange.

Ligand exchange with (D,L)-CYS: The SA stabilizers were exchanged with (D,L)-CYS molecules by a biphasic exchange method. Briefly, an aliquot of CdSe QDs were purified through three cycles of methanol addition and centrifugation. First, SA-stabilized CdSe QDs were dissolved in chloroform (2 mL) and mixed with (D,L)-CYS (40 mg mL^{-1}). The mixture was then stirred vigorously at 40 °C for 8 h until the chloroform solution was colorless. Thereafter, the aqueous solution was extracted and precipitated twice by the addition of methanol. Finally, CdSe QDs were redispersed in aqueous solution for CD and UV/Vis measurements.

Purification of CdTe or CdSe QDs for CD measurement: CdTe (or CdSe) QDs were firstly precipitated by centrifugating a mixture of 2-propanol (5 mL) and a solution of (D,L)-GSH- (or CYS)-stabilized CdTe QDs (5 mL) at 10000 rpm for 5 min. The precipitates were then dried under vacuum and kept in the dark under argon gas until use. Thereafter, QD solutions with desirable concentrations for CD measurement were prepared by redissolving solid QDs in different amounts of pure water. More detailed information of the purification procedure is described in the Supporting Information.

UV/Vis absorption spectroscopy (Hitachi U-3010) and photoluminescence spectroscopy (Horiba Jobin Yvon FM-4) were conducted to record the optical properties of CdTe or CdSe QDs at room temperature. The QD samples for spectral measurement were diluted with phosphate buffer solution (pH 7.4) until their absorption at 480 nm was below 0.1. CD spectra were recorded with a Jasco J-810 spectropolarimeter in aqueous solution. The measured photomultiplier voltage was between 170 V and 500 V, and the amplitudes of the absorption peaks of the QDs were kept below 1.2 to optimize the CD signals. All of the curves were averaged by five repeating measurements.

Received: June 2, 2011
Published online: October 6, 2011

Keywords: chirality · circular dichroism · quantum dots · size dependence

[1] a) A. P. Alivisatos, *Science* **1996**, *271*, 933 – 937; b) W. C. W. Chan, S. M. Nie, *Science* **1998**, *281*, 2016 – 2018; c) L. E. Brus, *J. Chem. Phys.* **1984**, *80*, 4403 – 4409.

[2] a) C. B. Murray, D. J. Norris, M. G. Bawendi, *J. Am. Chem. Soc.* **1993**, *115*, 8706 – 8715; b) N. Gaponik, D. V. Talapin, A. L. Rogach, K. Hoppe, E. V. Shevchenko, A. Kornowski, A. Eychmuller, H. Weller, *J. Phys. Chem. B* **2002**, *106*, 7177 – 7185; c) D. Y. Wang, A. L. Rogach, F. Caruso, *Nano Lett.* **2002**, *2*, 857 – 861; d) E. D. Sone, E. R. Zubarev, S. I. Stupp, *Angew. Chem.* **2002**, *114*, 1781 – 1785; *Angew. Chem. Int. Ed.* **2002**, *41*, 1705 – 1709.

[3] a) T. G. Schaaff, G. Knight, M. N. Shafigullin, R. F. Borkman, R. L. Whetten, *J. Phys. Chem. B* **1998**, *102*, 10643 – 10646; b) T. G. Schaaff, R. L. Whetten, *J. Phys. Chem. B* **2000**, *104*, 2630 – 2641; c) Y. S. Xia, Y. L. Zhou, Z. Y. Tang, *Nanoscale* **2011**, *3*, 1374 – 1382.

[4] a) M. P. Moloney, Y. K. Gun'ko, J. M. Kelly, *Chem. Commun.* **2007**, 3900 – 3902; b) S. D. Elliott, M. P. Moloney, Y. K. Gun'ko, *Nano Lett.* **2008**, *8*, 2452 – 2457; c) S. A. Gallagher, M. P. Moloney, M. Wojdyla, S. J. Quinn, J. M. Kelly, Y. K. Gun'ko, *J. Mater. Chem.* **2010**, *20*, 8350 – 8355; d) M. Naito, K. Iwahori, A. Miura, M. Yamane, I. Yamashita, *Angew. Chem.* **2010**, *122*, 7160 – 7163; *Angew. Chem. Int. Ed.* **2010**, *49*, 7006 – 7009.

[5] a) J. B. Pendry, *Science* **2004**, *306*, 1353 – 1355; b) I. Lieberman, G. Shemer, T. Fried, E. M. Kosower, G. Markovich, *Angew. Chem.* **2008**, *120*, 4933 – 4935; *Angew. Chem. Int. Ed.* **2008**, *47*, 4855 – 4857; c) Y. Y. Li, Y. L. Zhou, H. Y. Wang, S. Perrett, Y. L. Zhao, Z. Y. Tang, G. J. Nie, *Angew. Chem.* **2011**, *123*, 5982 – 5986; *Angew. Chem. Int. Ed.* **2011**, *50*, 5860 – 5864; d) J. M. Slocik, A. O. Govorov, R. R. Naik, *Nano Lett.* **2011**, *11*, 701 – 705; e) A. Guerrero-Martínez, B. Auguié, J. L Alonso-Gómez, Z. Džolić, S. Gómez-Graña, M. Žinić, M. M. Cid, L. M. Liz-Marzán, *Angew. Chem.* **2011**, *123*, 5613 – 5617; *Angew. Chem. Int. Ed.* **2011**, *50*, 5499 – 5503.

[6] N. A. Kotov, *Science* **2010**, *330*, 188 – 189.

[7] a) C. Gautier, T. Bürgi in *Chirality at the Nanoscale: Nanoparticles, Surfaces, Materials and more* (Ed.: D. B. Amabilino), Wiley, Hoboken, **2009**, chap. 3; b) C. Noguez, I. L. Garzon, *Chem. Soc. Rev.* **2009**, *38*, 757 – 771; c) P. J. Stephens, F. J. Devlin, C. F. Chabalowski, M. J. Frisch, *J. Phys. Chem.* **1994**, *98*, 11623 – 11627; d) I. L. Garzón, M. R. Beltran, G. Gonzalez, I. Gutierrez-Gonzalez, K. Michaelian, J. A. Reyes-Nava, J. I. Rodrguez-Hernandez, *Eur. Phys. J. D* **2003**, *24*, 105 – 109; e) M. R. Goldsmith, C. B. George, G. Zuber, R. Naaman, D. H. Waldeck, P. Wipf, D. N. Beratan, *Phys. Chem. Chem. Phys.* **2006**, *8*, 63 – 67.

[8] a) H. Yao, K. Miki, N. Nishida, A. Sasaki, K. Kimura, *J. Am. Chem. Soc.* **2005**, *127*, 15536 – 15543; b) P. D. Jadzinsky, G. Calero, C. J. Ackerson, D. A. Bushnell, R. D. Kornberg, *Science* **2007**, *318*, 430 – 433; c) J. George, K. G. Thomas, *J. Am. Chem. Soc.* **2010**, *132*, 2502 – 2503; d) T. Nakashima, Y. Kobayashi, T. Kawai, *J. Am. Chem. Soc.* **2009**, *131*, 10342 – 10343; e) Y. L. Zhou, M. Yang, K. Sun, Z. Y. Tang, N. A. Kotov, *J. Am. Chem. Soc.* **2010**, *132*, 6006 – 6013.

[9] a) A. O. Govorov, Z. Fan, P. Hernandez, J. M. Slocik, R. R. Naik, *Nano Lett.* **2010**, *10*, 1374 – 1382; b) Z. Y. Fan, A. O. Govorov, *Nano Lett.* **2010**, *10*, 2580 – 2587.

[10] N. Berova, K. Nakanishi, R. W. Woody in *Circular Dichroism: Principles and Applications*, 2nd ed., Wiley-VCH, New York, **2000**.

[11] a) B. T. Draine, *Astrophys J.* **1988**, *333*, 848 – 872; b) C. E. Román-Velázquez, C. Noguez, I. L. Garzón, *J. Phys. Chem. B* **2003**, *107*, 12035 – 12038.

[12] J. Y. Quyang, M. B. Zaman, F. J. Yan, D. Johnston, G. Li, X. Wu, D. Leek, C. I. Ratcliffe, J. A. Ripmeester, K. Yu, *J. Phys. Chem. C* **2008**, *112*, 13805 – 13811.

